Electronic Supplementary Material (ESI) for Nanoscale
This journal is © Royal Society of Chemistry 2018

Supplementary Information

Stabilizing the Structure of $LiMn_{0.5}Fe_{0.5}PO_4$ via Formation of Concentration-gradient Hollow Spheres with Fe-rich Surfaces

Tingting Ruan,[a] Bo Wang,*[a, b] Fei Wang,[a] Rensheng Song,[a] Fan Jin,[a] Yu Zhou,[b] Dianlong Wang,*[a] Shixue Dou[c]

[a] *MIIT Key Laboratory of Critical Materials Technology for New Energy Conversion and Storage, School of Chemistry and Chemical Engineering, Harbin Institute of Technology, 150001 Harbin, China.*

[b] *School of Materials Science and Engineering, Harbin Institute of Technology, 150001 Harbin, China.*

[c] *Institute for Superconducting & Electronic Materials, Australian Institute of Innovative Materials, University of Wollongong, Wollongong, NSW 2500, Australia.*

∗ *Corresponding author. Fax: +86 45186413721; Tel: +86 45186413751.*

E-mail address:

wangdianlonghit@163.com (D. L. Wang)

wangbo19880804@163.com (B. Wang)

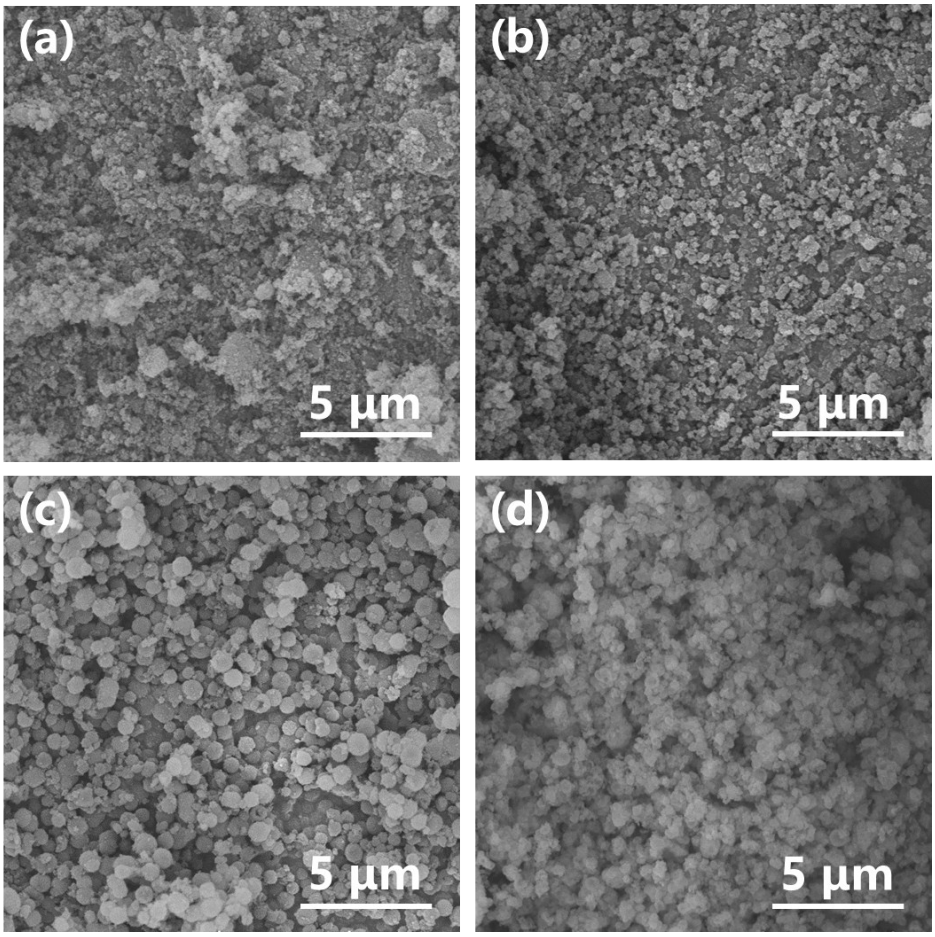

Figure S1† SEM images of the Li_3PO_4 particles obtained with different volume ratios of H_2O:PEG600: a) 1:2, b) 3:2, c) 3:1, d) 5:0.

As can be seen from the scanning electron microscope (SEM) images, the particle size of the Li_3PO_4 became larger and a spherical morphology was formed as the H_2O:PEG600 solvent ratio was raised from 1:2 to 3:1, which could be attributed to the different velocities influencing the mass transport for the synthesis reaction. As the volume ratio of H_2O to PEG600 grew higher, the viscosity of the solution decreased, which would expedite the mass transfer process for the nucleation and growth of Li_3PO_4 spheres. The resulting Li_3PO_4 nanoparticles would create rough surface, however, and stick together in the absence of PEG600, as it manifested a strong capping effect on Li_3PO_4 surface. The adsorption of PEG600 could reduce the surface energy of Li_3PO_4, which consequently overcame the tendency of particles towards fusion with each other.[1]

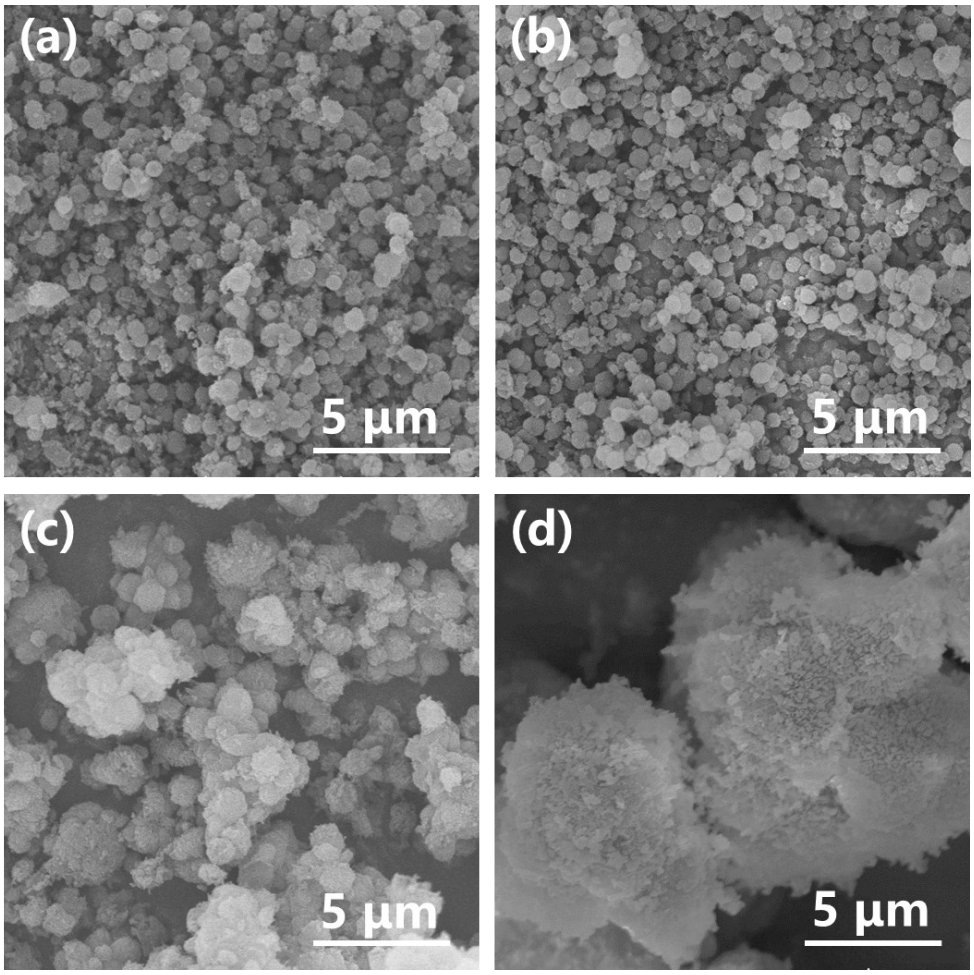

Figure S2† SEM images of the Li_3PO_4 particles obtained at different pH values: a) pH = 10, b) pH = 11, c) pH = 13, d) pH = 14.

As shown in **Fig. S2**, as the pH value of the original solution increased, the hollow spherical structure of Li_3PO_4 vanished and the particles were agglomerated into large grains, due to the dominance of PO_4^{3-} at higher pH values without the pre-sacrificial precipitation of Li_2HPO_4, turning the hollow structured spheres into large solid ones.

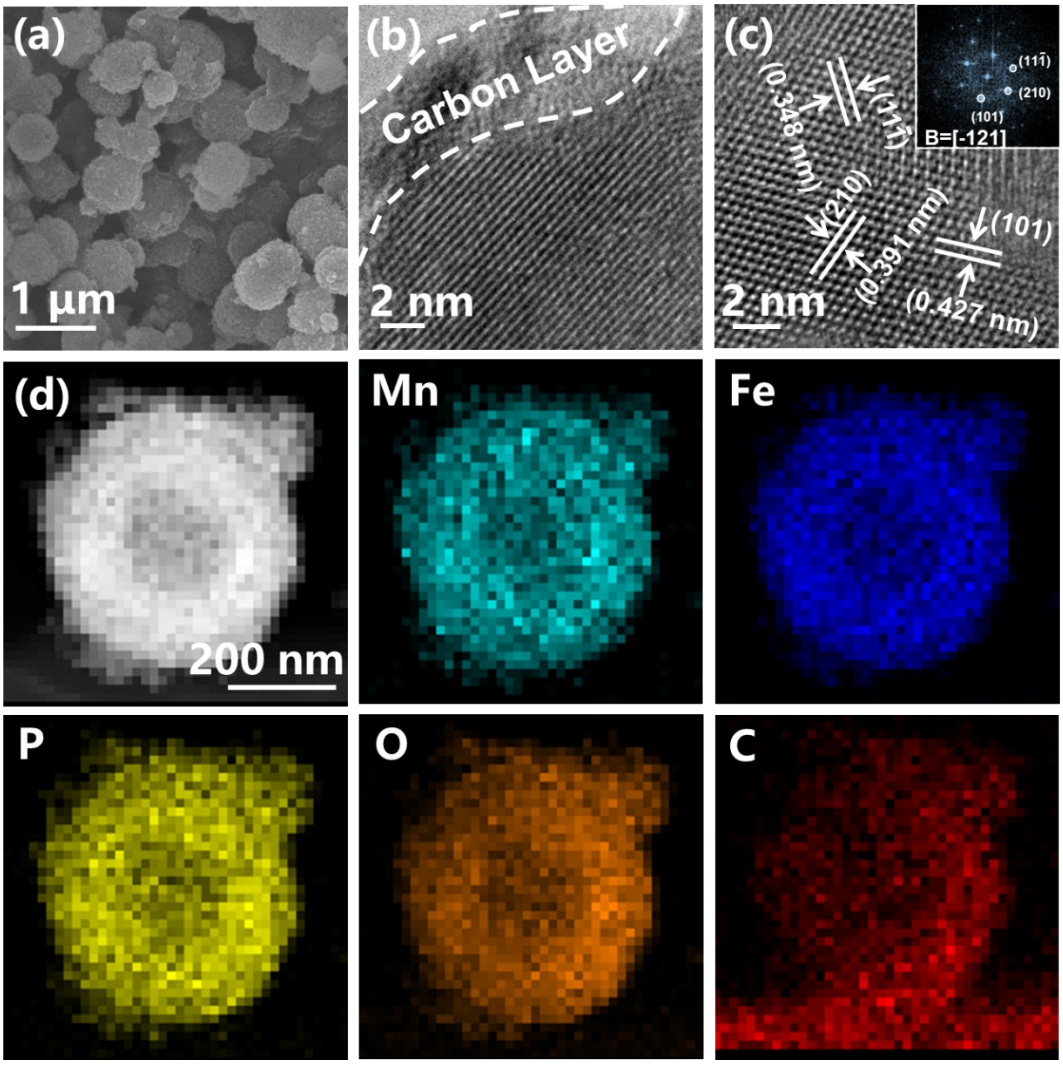

Figure S3† a) SEM image of C-LMFP/C. b, c) HRTEM images of C-LMFP/C with FFT pattern in the inset of c). d) HAADF-STEM image and elemental mapping results from a cross-section of a C-LMFP/C sphere.

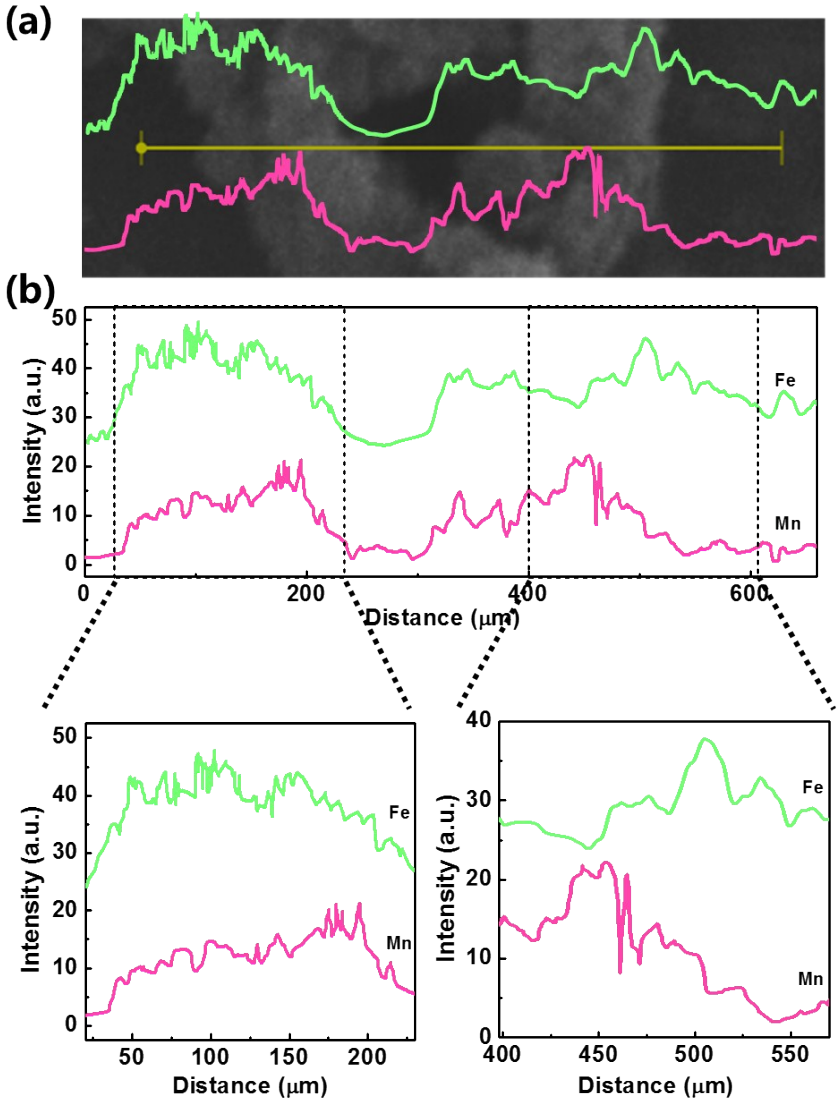

Figure S4† a) SEM image of a broken HCG-LMFP/C sphere. b) Line scan profiles of Fe and Mn across a broken HCG-LMFP/C sphere.

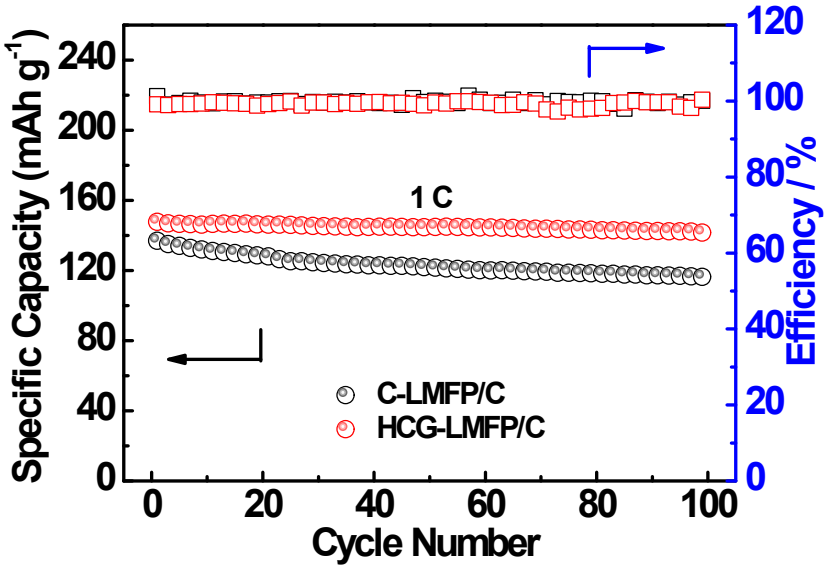

Figure S5† Cycling performances of C-LMFP/C and HCG-LMFP/C at the 1C rate.

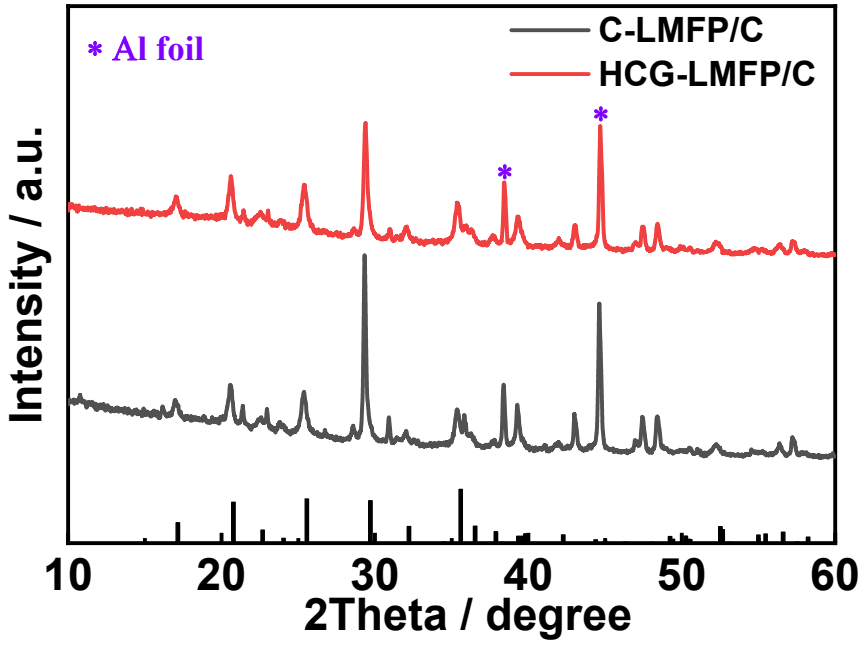

Figure S6† XRD patterns of C-LMFP/C and HCG-LMFP/C after cycling.

Table S1† Lattice constants and unit cell volume from the Rietveld refinements of C-LMFP and HCG-LMFP samples. R_p: profile R-factor; R_{wp}: weighted profile R-factor; χ^2: goodness-of-fit parameter.

Samples	a/Å	b/Å	c/Å	V/Å^3	R_{wp}/%	R_p/%	χ^2
C-LMFP/C	10.3285	6.0140	4.6945	291.60	3.01	2.47	1.52
HCG-LMFP/C	10.3216	6.0109	4.6926	291.14	2.75	2.18	1.46

Table S2† Comparison of the properties in the present work with other $LiMnPO_4$-$LiFePO_4$ related cathodes reported in the last three years.

Composites	Particle size	Electrochemical behavior	References
$LiFePO_4$ nanoplatelets wrapped in a nitrogen-doped grapheme aerogel	~200 nm in length, ~40 nm in thickness	Initial discharge capacity ~124 mAh g^{-1}, with a capacity retention of 89% after 1000 cycles at 10C rate	2
$LiMn_{0.5}Fe_{0.5}PO_4$ nanoparticles	~50 nm	Initial discharge capacity ~109 mAh g^{-1}, with a capacity retention of 90% after 100 cycles at 1C rate	3
Mesoporous $LiMnPO_4$ nanoplates	~200 nm in length, 5-20 nm in thickness	Initial discharge capacity ~156 mAh g^{-1}, with a capacity retention of 83% after 100 cycles at 1C rate	4
$LiMn_{0.75}Fe_{0.25}PO_4$ nanoplates with fluorine-doped carbon coating	~150 nm	discharge capacity ~120 mAh g^{-1} at the 500th cycle at 10C rate, with a capacity retention of 80%	5
$LiMn_{0.6}Fe_{0.4}PO_4$	Unmentioned	discharge capacity ~90 mAh g^{-1} at the 1000th cycle at 10C rate	6
$LiFePO_4$ nanosheets	~5 μm in lateral size, 15-20 nm in thickness	discharge capacity ~120 mAh g^{-1} at the 500th cycle at 5C rate, with a capacity retention of 93%	7
$LiFePO_4$ nanoplatelets	80-100 nm in length, 40-60 nm in width, 10-20 nm in thickness	discharge capacity ~105 mAh g^{-1} at the 1000th cycle at 10C rate, with a capacity retention of 87%	8
$LiMn_{0.9}Fe_{0.1}PO_4$-polyacene	unmentioned	discharge capacity ~91 mAh g^{-1} at the 100th cycle at 10C rate, with a capacity retention of 89.7%	9
$LiMn_{0.8}Fe_{0.2}PO_4$ microspheres	~1 μm in diameter	discharge capacity ~105 mAh g^{-1} at the 1000th cycle at 5C rate, with a capacity retention of 93.9%	10
$LiMn_{0.65}Fe_{0.35}PO_4$ at core covered by $LiMn_{0.38}Fe_{0.62}PO_4$ with an average composition of $LiMn_{0.5}Fe_{0.5}PO_4$	~600 nm	Initial discharge capacity ~117 mAh g^{-1}, with a capacity retention of 96% after 1000 cycles at 1C rate	This work

Table S3† Results for the charge process in HCG-LMFP/C.

Current densities	0.1C	0.2C	1C	2C	5C	10C	20C	60C
galvanostatic charge capacity (mAh g^{-1})	168.10	156.40	147.42	137.04	128.09	110.12	93.5	60.0
Total capacity (mAh g^{-1})	168.12	156.43	147.59	138.0	131	117.2	103	72.76
galvanostatic charge capacity fraction (%)	99.98	99.97	99.88	99.31	97.78	93.96	90.29	82.47

Table S4† Results for the charge process in C-LMFP/C.

Current densities	0.1C	0.2C	1C	2C	5C	10C	20C	60C
galvanostatic charge capacity (mAh g^{-1})	169.32	156.17	146.26	126.54	101.64	75.74	53.85	21.60
Total capacity (mAh g^{-1})	169.34	156.21	146.51	127.58	104	85.6	66.7	35.13
galvanostatic charge capacity fraction (%)	99.98	99.97	99.83	99.19	97.72	88.49	80.74	61.48

Table S5† The structure parameters of the C-LMFP/C and HCG-LMFP/C cathodes after cycling.

Samples		C-LMFP/C	HCG-LMFP/C
Space group		*Pnma* (orthorhombic)	*Pnma* (orthorhombic)
Unit cell parameters	Cell volume (Å^3)	296.22	292.92
	a (Å)	10.3975	10.3944
	b (Å)	6.0281	6.0235
	c (Å)	4.7262	4.6782

Table S6† The structure parameters of the $LiMnPO_4$, $MnPO_4$, $LiFePO_4$, and $FePO_4$ samples.

Samples		$LiMnPO_4$	$LiFePO_4$	$MnPO_4$	$FePO_4$
Space group		*Pnma* (orthorhombic)	*Pnma* (orthorhombic)	*Pnma* (orthorhombic)	*Pnma* (orthorhombic)
Unit cell parameters	Cell volume ($Å^3$)	310.8783	302.4183	275.8838	290.6502
	a (Å)	10.5751	10.4529	9.7575	10.0089
	b (Å)	6.1570	6.0864	5.8580	5.9326
	c (Å)	4.7746	4.7534	4.8265	4.8647
M-O parameters	Average bond length (Å)	2.2193	2.1841	2.0327	2.0623
	Distortion index (Å)	0.0278	0.0339	0.0626	0.0399

References

1. S.-L. Yang, R.-G. Ma, M.-J. Hu, L.-J. Xi, Z.-G. Lu and C. Y. Chung, *J Mater Chem*, 2012, **22**, 25402.

2. B. Wang, W. Al Abdulla, D. Wang and X. S. Zhao, *Energ Environ Sci*, 2015, **8**, 869-875.

3. W. Xiang, Y. J. Zhong, J. Y. Ji, Y. Tang, H. Shen, X. D. Guo, B. H. Zhong, S. X. Dou and Z. Y. Zhang, *Physical chemistry chemical physics : PCCP*, 2015, **17**, 18629-18637.

4. F. Wen, H. Shu, Y. Zhang, J. Wan, W. Huang, X. Yang, R. Yu, L. Liu and X. Wang, *Electrochim Acta*, 2016, **214**, 85-93.

5. X. Yan, D. Sun, Y. Wang, Z. Zhang, W. Yan, J. Jiang, F. Ma, J. Liu, Y. Jin and K. Kanamura, *Acs Sustain Chem Eng*, 2017, **5**, 4637-4644.

6. S. Li, X. Meng, Q. Yi, J. A. Alonso, M. T. Fernández-Díaz, C. Sun and Z. L. Wang, *Nano Energy*, 2018, **52**, 510-516.

7. L. L. Peng, X. Zhang, Z. W. Fang, Y. Zhu, Y. J. Xie, J. J. Cha and G. H. Yu, *Chem Mater*, 2017, **29**, 10526-10533.

8. B. Wang, A. M. Liu, W. Al Abdulla, D. L. Wang and X. S. Zhao, *Nanoscale*, 2015, **7**, 8819-8828.

9. L. G. Wang, P. J. Zuo, G. P. Yin, Y. L. Ma, X. Q. Cheng, C. Y. Du and Y. Z. Gao, *J Mater Chem A*, 2015, **3**, 1569-1579.

10. P. J. Zuo, L. G. Wang, W. Zhang, G. P. Yin, Y. L. Ma, C. Y. Du, X. Q. Cheng and Y. Z. Gao, *Nanoscale*, 2015, **7**, 11509-11514.